

SEVENTH FRAMEWORK PROGRAMME
CAPACITIES - ERA.Net RUS: Linking Russia to the ERA

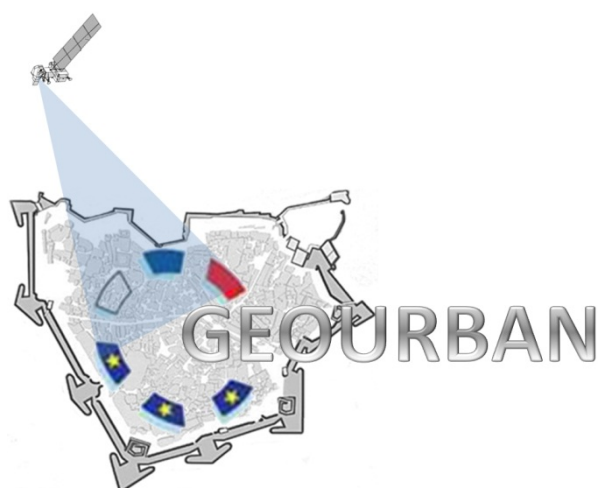


Contract for:

Innovation Project

D.3

EO-based Indicators Development



Project acronym: **GEOURBAN**

Project full title: **ExploitinG
Earth Observation in
sUstainable uRBan
plAnning & maNagement**

Contract no.: **ERA.Net-RUS-033**

Date: **22/07/2013**

Doc.Ref.: **GEOURBAN_36_TR_FORTH**

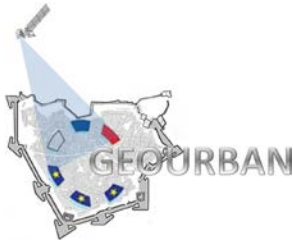
Book Captain: **Dimitrios Triantakostas**

Contributors: **Nektarios Chrysoulakis**

Issue: **1.0**

Deliverable no.: **D.3**

Dissemination: **RE**



GEOURBAN

**WP3: EO-based indicators
development**

Deliverable no.: D.3
Contract no.: ERA.Net-RUS-033
Document Ref.: GEOURBAN_36_TR_FORTH
Issue: 1.0
Date: 30/08/2013
Page number: 2/39

Document Status Sheet

Issue	Date	Author	Comments
0.0	15/05/2013	D. Triantakonstantis	Draft out for consortium review
0.1	15/07/2013	N. Chrysoulakis	Review
1.0	30/08/2013	D. Triantakonstantis N. Chrysoulakis	Version 1.0 delivered to JCS

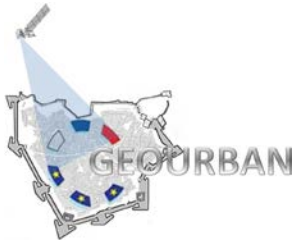
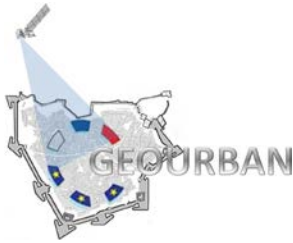


Table of Contents

DOCUMENT STATUS SHEET	2
TABLE OF CONTENTS	3
1. WORKPACKAGE OVERVIEW	4
1.1. PURPOSE OF THE DOCUMENT	4
1.2. DOCUMENT REFERENCES.....	5
2. EO-BASED URBAN INDICATORS	9
2.1. INTRODUCTION	9
2.2. URBAN SURFACE STRUCTURE	15
2.2.1. DENSITY INDICATORS	15
2.2.1.1. BUILT-UP DENSITY	15
2.2.1.2. TERRASAR-X BUILDING DENSITY (TSX-BUILDING).....	17
2.2.1.3. OPEN SPACE DENSITY (OSD).....	18
2.2.1.4. GREEN SPACE DENSITY (GSD).....	19
2.2.2. AREA / EDGE INDICATORS	20
2.2.2.1. EDGE DENSITY (ED)	21
2.2.3. RATIO INDICATORS.....	22
2.2.3.1. IMPERVIOUSNESS-OPEN SPACE RATIO (IOR).....	22
2.2.3.2. IMPERVIOUSNESS-GREEN SPACE RATIO (IGR)	23
2.2.4. DIVERSITY INDICATORS	24
2.2.4.1. CLASS RICHNESS DENSITY (CRD).....	24
2.2.4.2. ECOLOGICAL EFFECTIVENESS RATIO (EER).....	25
2.3. URBAN SURFACE TYPE.....	27
2.3.1. IMPERVIOUSNESS	27
2.3.2. FRACTIONAL LAND COVER	28
2.3.3. SURFACE ALBEDO.....	29
2.3.4. SURFACE EMISSIVITY.....	31
2.4. URBAN SPRAWL.....	32
2.4.1. URBAN FRINGE.....	32
2.4.2. SCATTER DEVELOPMENT (SD).....	33
2.4.3. CHANGE DETECTION	34
2.5. URBAN ENVIRONMENTAL QUALITY	35
2.5.1. SURFACE URBAN HEAT ISLAND	35
2.5.2. AEROSOL OPTICAL THICKNESS (AOT).....	37
2.6. VULNERABILITY TO HAZARDS.....	38
2.6.1. ACCESSIBILITY TO CRITICAL SERVICES.....	38
2.7. SOCIOECONOMICS.....	38
2.7.1. EXPOSURE TO PM.....	38

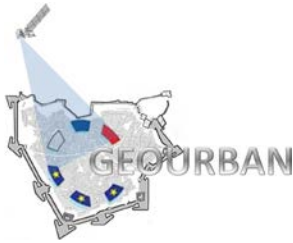


1. WORKPACKAGE OVERVIEW

WP3 is a central WP in GEOURBAN, because the main research activity focuses on the development of urban indicators. It is the result of the synthesis of several Earth Observation (EO) products at various scales in a way that they result in meaningful information for urban planning and management. They will have the potential to provide urban planners with meaningful information related to the monitoring of urban sprawl (track urban area growth and change, monitor changes in peri-urban regions), mapping and analyzing the urban surface structure (land cover, buildings arrangement, assess the spatial arrangement of green/open space within cities and at the periphery), extracting of bio-physical parameters (albedo, emissivity, impervious areas), assessing urban environmental and microclimatic characteristics (track land-cover and land-use changes that influence urban climatology and atmospheric deposition, urban heat island and air quality monitoring) and assessing urban vulnerability to natural disaster risks (earthquakes, subsidence, mudslides, floods) and urban security (crime prevention through urban planning). The indicators support decision-making to optimize the planning and management in the urban environment through the use of the Web-based Information System (WIS). The output of this WP is a set of indicators to be used by the GEOURBAN WIS and a report summarizing the development of these indicators. **WP3** contiguously interacts with **WPs 2,4, 5 and 6** and give inputs to **WPs 7 and 9**. **FORTH** leads WP3; KUZGUN, DLR and UNIBAS participate.

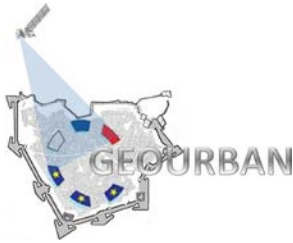
1.1. Purpose of the document

This document is the GEOURBAN deliverable **D.3: Earth Observation-based Indicators Development**. It provides the required information about urban indicators development. More specifically, it includes a description of each indicator and the conceptual algorithm needed its evaluation from EO data. These algorithms have been implemented in the WIS in the framework of WP7.

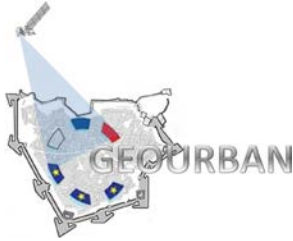


1.2. Document references

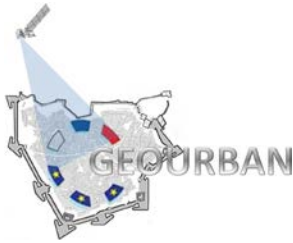
1. Adams, J. B., Sabol, D. E., Kapos, V., Almeida Filho, R., Dar A. Roberts, Smith, M. O. and Gillespie, A. R. 1995. Classification of multispectral images based on fractions of endmembers: Application to land-cover change in the Brazilian Amazon, *Remote Sensing of Environment* 52 (2), pages: 137-154.
2. Afify, H. A. 2011. Evaluation of change detection techniques for monitoring land-cover changes: A case study in new Burg El-Arab area. *Alexandria Engineering Journal* 50 (2), pages: 187-195.
3. Benas, N., Beloconi, A. and Chrysoulakis, N. 2013. Estimation of urban PM10 concentration, based on MODIS and MERIS/AATSR synergistic observations. *Atmospheric Environment* 79, pages: 448-454.
4. Bhatta, B., Saraswati, S. and Bandyopadhyay, D. 2010. Quantifying the degree of freedom, degree of sprawl, and degree of goodness of urban growth from remote sensing data. *Applied Geography* 30, pages: 96-111.
5. Brander, L. M. and Koetse, M. J. 2011. The value of urban open space: Meta-analyses of contingent valuation and hedonic pricing results, *Journal of Environmental Management* 92 (10), pages: 2763-2773.
6. Briassoulis, H. 2001. Sustainable development and its indicators: through a (planner's) glass darkly. *Journal of Environmental Planning and Management*, 44 (3), pages: 409-427.
7. Carlson, T.N., Ripley, D.A., 1997. On the relation between NDVI, fractional vegetation cover, and leaf area index. *Remote Sensing of Environment*, 62, pages: 241-252.
8. CEC, 2006. Cohesion Policy and Cities: the urban contribution to growth and jobs in the regions, Communication from the Commission to the council and parliament, COM(2006) 385, final, Brussels, Belgium, July 13th.
9. CEC, 2011. Territorial Agenda of the European Union 2020: towards an inclusive, smart and sustainable Europe of diverse regions, Hungary, May 19th.
10. Esch, T., Taubenbock, H., Heldens, W., Thiel, M., Wurm, M. and Deck, S. 2010. Urban remote sensing: How can earth observation support the sustainable



- development of urban environments? Urban Remote Sensing, 46th ISOCARP Congress.
11. Ewing, R.H. 2008. Characteristics, Causes and Effects of Sprawl: A Literature Review. *Urban Ecology*, pages: 519-535.
 12. Herold, M., Liu, X. and Clarke, K. C. 2003. Spatial metrics and image texture for mapping urban land use. *Photogrammetric Engineering and Remote Sensing* 69, pages: 991–1001.
 13. Herzele, A. V. and Wiedemann, T. 2003. A monitoring tool for the provision of accessible and attractive urban green spaces, *Landscape and Urban Planning* 63 (2), pages 109-126.
 14. Ji, W., Ma, J., Twibell, R. W. and Underhill, K. 2006. Characterizing urban sprawl using multi-stage remote sensing images and landscape metrics, *Computers, Environment and Urban Systems* 30 (6), pages 861-879.
 15. Kasanko, M., Barredo, J. I., Lavalle, C., McCormick, N., Demicheli, L., Sagris, V. and Brezger, A. 2006. Are European cities becoming dispersed?: A comparative analysis of 15 European urban areas, *Landscape and Urban Planning* 77 (1–2), pages 111-130.
 16. Liang, S., 2000. Narrowband to broadband conversions of land surface albedo: I. Algorithms. *Remote Sensing of Environment* 76, pages 213-238.
 17. Liang, S. et al., 2002. Narrowband to broadband conversions of land surface albedo: II. Validation. *Remote Sensing of Environment* 84, pages 25-41.
 18. Lu, D. and Weng, Q. 2006. Use of impervious surface in urban land-use classification, *Remote Sensing of Environment* 102 (1–2), pages 146-160.
 19. Lakes, T. and Kim, H. O. 2012. The urban environmental indicator “Biotope Area Ratio”—An enhanced approach to assess and manage the urban ecosystem services using high resolution remote-sensing, *Ecological Indicators* 13 (1), pages 93-103.
 20. Masser, I. 2001. Managing our urban future: The role of remote sensing and geographical information systems. *Habitat International* 0, pages 1-10.
 21. Melesse, A. M. Weng, Q., Thenkabail, P. S., Senay, G. B. 2007. Remote Sensing Sensors and Applications in Environmental Resources Mapping and Modelling, *Sensors* 7 (12), pages: 3209-3241.



22. Mitraka, Z., Chrysoulakis, N., Kamarianakis, Y., Partsinevelos, P. and Tsouchlaraki, A. 2012. Improving the estimation of urban surface emissivity based on sub-pixel classification of high resolution satellite imagery, *Remote Sensing of Environment* 117, pages 125-134.
23. Ridd, M. K. and Liu, J. 1998. A comparison of four algorithms for change detection in an urban environment. *Remote Sensing of Environment* 63 (2), pages: 95-100.
24. Salisbury, J. W. and D'Aria, D. M., 1992, Emissivity of terrestrial materials in the 8-14 μm atmospheric window: *Remote Sensing of Environment* 42, pages: 83-106.
25. Singh, A. 1989. Digital change detection techniques using remotely-sensed data. *International Journal of Remote Sensing* 10 (6), pages: 989-1003.
26. Sobrino, J. A., Jiménez-Muñoz, J. C., Paolini, L. 2004. Land surface temperature retrieval from LANDSAT TM 5, *Remote Sensing of Environment*, 89, pages: 467–483.
27. Pauleit, S. and Duhme, F. 2000. Assessing the environmental performance of land cover types for urban planning. *Landscape and Urban Planning* 52 (1), pages 1-20.
28. Shen, L. Y., Ochoa, J. J., Shah, M. N. and Zhang, X. 2011. The application of urban sustainability indicators – a comparison between various practices. *Habitat International* 35, pages: 17-29.
29. Tran, H., Daisuke, U., Shiro, O. and Yoshifumi, Y. 2006. Assessment with satellite data of the urban heat island effects in Asian mega cities. *International Journal of Applied Earth Observation and Geoinformation* 8, pages: 34-48.
30. Yang, X. and Liu, Z. 2005. Use of satellite-derived landscape imperviousness index to characterize urban spatial growth. *Computers, Environment and Urban Systems* 29 (5), pages 524-540.
31. Yin, Z. Y., Stewart, D. J., Bullard, S. and MacLachlan, J. T. 2005. Changes in urban built-up surface and population distribution patterns during 1986–1999: A case study of Cairo, Egypt. *Computers, Environment and Urban Systems* 29 (5), pages: 595-616.
32. Wan, Z., Zhang, Y., Zhang, Q., Li, Z.L., 2004. Quality assessment and validation of the MODIS global land surface temperature. *Int. J. Remote Sensing* 10, pages: 261-274.

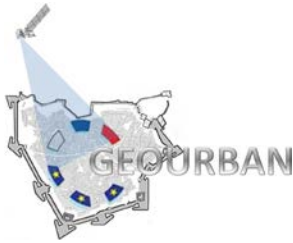


GEOURBAN

WP3: EO-based indicators development

Deliverable no.: D.3
Contract no.: ERA.Net-RUS-033
Document Ref.: GEOURBAN_36_TR_FORTH
Issue: 1.0
Date: 30/08/2013
Page number: 8/39

-
33. Wassmer, R., 2000. Urban sprawl in a U.S. metropolitan area: Ways to measure and a comparison of the Sacramento area to similar metropolitan areas in California and the U.S., September 8. CSUS Public Policy and Administration Working Paper No. 2000-03, pages: 22.
 34. Werninghaus, R. 2004. TerraSAR-X mission. Proceedings SPIE 5236, SAR Image Analysis, Modeling, and Techniques VI, 9 (January 12, 2004).



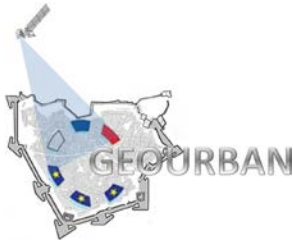
2. EO-based Urban Indicators

2.1. Introduction

Cities attract the interest of world scientific and planning community due to their accelerating growth of residential population. In 2007 the urban population was outnumbered the rural population for the first time in history and two thirds of the world's population is estimated to live in cities by 2030 (UNPP 2008). Cities become the center of cultural, economical and political development and therefore, any expert intervention for a sustainable living experience would improve the quality of life. EO is one of the main fields of research, which can provide powerful tools in urban management and planning. Nowadays, EO can be used to analyze urban surface structure, physiognomy, traffic, land uses and building density quickly and accurately. This information appears to be valuable inputs in urban management and planning, which require data methods and tools for evaluating alternatives in decision making.

EO data derived from spaceborn and airborne systems have become promising sources of geoinformation, valuable in many urban applications (Masser 2001; Bhatta et al. 2010; Esch et al. 2010). Data from a large number of sensors are available to urban studies. This data are acquired in different spatial, spectral and temporal resolution. The different characteristics of EO data allow different applications such as land cover mapping and change detection, urban morphology characterization, surface energy balance estimation, air quality and thermal stress assessments. According to different spatial resolution, the following categories can be specified:

1. At low and medium spatial resolution (MR), global urban maps are generated by using imagery collected from optical sensors as MODIS (NASA, 2013a), DMSP-OLS (NOAA, 2013a), AVHRR (NOAA, 2013b), MERIS (ESA, 2013a), SPOT-4-VEGETATION (CNES, 2013). In this context, so far MODIS 500 and GlobCover 2009 products, are the two most accurate settlements layers available worldwide with a spatial resolution of 493 and 309 meters, respectively (Potere et al., 2009).
2. At city to local scale, high spatial resolution (HR) data are typically used for regional analyses including thematic characterization of major urban types. In such framework, both optical (e.g., Landsat TM and ETM+ (NASA, 2013b), SPOT (CNES,



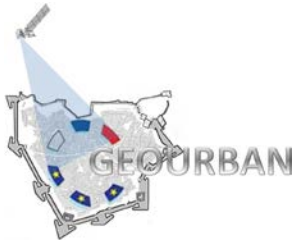
2013), IRS LISS and AWiFS (ISRO, 2013), as well as radar sensors (e.g., TerraSAR-X (DLR, 2013a), TanDEM-X (DLR, 2013b), RADARSAT (CSA, 2013), ALOS-PALSAR (JAXA, 2013), Cosmo SkyMed (UGS, 2013) are generally employed with a spatial resolution ranging from 10 to 50 m.

3. Local-scale analyses are carried out by means of very high resolution data (VHR) acquired by optical systems - e.g., RapidEye (RapidEye, 2013), CARTOSAT (ISRO, 2013), IKONOS (DigitalGlobe, 2013), QuickBird (DigitalGlobe, 2013), WorldView 1 and 2 (DigitalGlobe, 2013), GeoEye 1 and 2 (DigitalGlobe, 2013) - or radar satellites such as TerraSAR-X (DLR, 2013a), TanDEM-X (DLR, 2013b), or RADARSAT (CSA, 2013). The spatial resolution up to ~0.4 m allows a fine characterization of urban areas with high spatial detail.

Furthermore, using digital surface models derived from stereo imagery of VHR optical sensors such as CARTOSAT-1 or WorldView II, it became even possible to map complex urban environments in 3D. New perspectives with respect to the characterization of building volumes, although at a coarser resolution, are expected by the TanDEM-X.

EO urban indicators are powerful tools in describing urbanization process. They belong to a wider category, called urban sustainability indicators, which their aim is to understand the urban sustainability performance within an environmental, social and economical framework (Briassoulis, 2001; Shen et al. 2011). The great importance of EO urban indicators is based on its ability of easy and quick retrieval by EO data. Therefore, urban indicators become valuable means in planners' hands, because of their contribution to analyze and characterize urban form and shape, urban dynamics and urban microclimate. In Table 1, a preliminary list conducted by GEOURBAN Consortium is given. In this Table, the following information is listed: the indicators category, the name of indicators, the primary EO derived parameters (products) from which the indicators will be extracted, the study areas in which they will be estimated, the priority according to the planners' needs and finally the spatial resolution of data from which they will be calculated. With red color the priority for each particular city is depicted, whereas with the darkest the yellow color, the highest the priority for all GEOURBAN case studies.

Therefore, the following schema was considered: EO data – products – indicators. For example, multispectral data is the EO data recording by a satellite sensor. A land cover



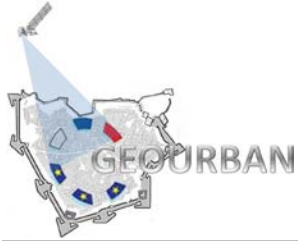
GEOURBAN

WP3: EO-based indicators development

Deliverable no.: D.3
Contract no.: ERA.Net-RUS-033
Document Ref.: GEOURBAN_36_TR_FORTH
Issue: 1.0
Date: 30/08/2013
Page number: 11/39

map can be produced as a product by this EO data using a supervised classification method. Furthermore, the building density indicator can be derived by land cover product by calculating the proportion of the built up areas compared to the total area within a specific administrative boundary.

In the following sections, the EO-based indicators which were selected and developed in GEOURBAN are presented. These indicators have been implemented in the WIS.



GEOURBAN

Category	Indicator	Primary EO derived parameters	Basel	Tel Aviv	Tyumen	PRIORITY	Spatial Resolution		
							VHR	HR	LR
Urban Surface Structure	Open spaces	Land cover					*	*	
	Green spaces	Land cover					*	*	
	Built-up density	Land cover, DSM					*		
	Building density	DSM					*		
	Building volume	DSM					*		
Urban Surface Type	Imperviousness	Fractional land cover, surface materials					*	*	*
	Vegetation fraction	Fractional land cover					*	*	
	Surface albedo	Albedo					*	*	*
	Surface emissivity	Emissivity					*	*	*
	urban forms (plane aspect ratio, canyon height/width ratio, plane area fraction, sky view factors)	DSM					*		
	Surface materials	spectral features					*		
	Land cover type	Land cover, material-based land cover					*	*	



GEOURBAN

WP3: EO-based indicators development

Deliverable no.: D.3
 Contract no.: ERA.Net-RUS-033
 Document Ref.: GEOURBAN_36_TR_FORTH
 Issue: 1.0
 Date: 30/08/2013
 Page number: 13/39

Category	Indicator	Primary EO derived parameters	Basel	Tel Aviv	Tyumen	PRIORITY	Spatial Resolution		
							VHR	HR	LR
Urban Sprawl	Land cover change	Land cover						*	
	Built-up density change	Land cover, DSM					*		
	Building volume change	Land cover, DSM					*		
	Surface albedo change	Albedo						*	*
	Contagion Index change	Land cover						*	
Urban Environmental Quality	Urban heat island intensity	Surface temperature, emissivity and albedo						*	*
	Aerosols concentration	AOT					*		*
	Urban landscape fragmentation	Land cover					*	*	
	GHG (CO2, N2O, CH4)	IPDA (Integrated path differential absorption)							
	solar irradiance, shadows	DSM					*		
	snow cover	land cover, albedo					*	*	*
	Urban vegetation fraction, urban greenness	Fractional land cover					*	*	



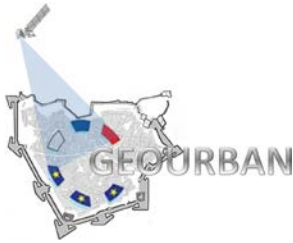
GEOURBAN

WP3: EO-based indicators development

Deliverable no.: D.3
 Contract no.: ERA.Net-RUS-033
 Document Ref.: GEOURBAN_36_TR_FORTH
 Issue: 1.0
 Date: 30/08/2013
 Page number: 14/39

Category	Indicator	Primary EO derived parameters	Basel	Tel Aviv	Tyumen	PRIORITY	Spatial Resolution		
							VHR	HR	LR
Vulnerability to Hazards	Surface topography	DTM						*	
	Built-up density	Land cover, DSM					*		
	Population distribution	Land cover, DSM					*		
	Dispersion	DSM, dispersion models							
	Accessibility	Land cover, street and railway network (geodata, visual interpretation)					*	*	
	Ground subsidence	Land deformation, DTM, InSAR					*		
	Critical infrastructure	Visual Interpretation					*		
Socioeconomics	Land use	Land cover					*	*	
	Population distribution	Land cover, DSM					*		
	Access to green areas	land cover					*	*	
	traffic	land cover, urban surface materials					*	*	
	Exposure to PM2.5	Land cover, DSM, AOT					*		*
various	Asbestos	urban surface materials					*		
	LOC	lines of communication (roads, railway, water)					*		
	CO ₂ balance, photosynthesis	DSM, spectral features, models							*
	CO, NO ₂ , Nox, Benzole, SO ₂ , H ₂ CO, Pb, Benzylene	DSM, spectral features, models							*

Table 1. Preliminary list of urban indicators



2.2. Urban Surface Structure

The urban surface structure indicators are extracted from land cover map products, using administrative political community boundaries, or user-defined boundaries (polygons). The value of each indicator is estimated using a dedicated formula within each polygon. The urban surface structure indicators estimated in GEOURBAN are: a) Density indicators (Built-up density, TerraSAR-X building density, Open Space Density and Green Space Density), b) Area / Edge indicators (Edge Density), c) Ratio indicators (Imperviousness-Open space ratio, Imperviousness-Green space ratio) and d) Diversity indicators (Class Richness Density and Ecological Effectiveness Ratio).

2.2.1. Density Indicators

2.2.1.1. Built-up density

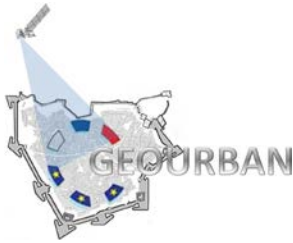
Built up density refers to the density of built-up areas (impervious areas). In these areas the infiltration of water is prevented. As a sum of impermeable landscape features, including buildings, roads, parking lots etc., built up density is a key indicator for addressing many environmental issues such as water quality and urban biodiversity (Yang and Liu, 2005).

Extensive research has been conducted to map built-up density using remote sensing techniques. In GEOURBAN, after producing land cover maps by employing EO image classification methods (as it has been described in Deliverables 4.2 and 5.2), the built-up density is calculated using the percentage of urban land cover which it is included within polygons defined by the user or by administrative political boundaries. The aim of this indicator is based on the need of urban planning in having a measurement of built-up areas within specific geographic entities. Therefore, the built-up density is the proportion of built-up areas within the area boundary. The land uses (and therefore the respective land cover classes produced in GEOURBAN) which are characterized as built-up areas are:

Residential I: high density

Residential II: medium density

Residential III: low density



GEOURBAN

Industrial/commercial

Low values of built-up density indicate large areas where water can be infiltrated, while large values belong to areas with large built-up cover.

$IMP = \frac{N}{A} * 100$	<p>N = number of built-up areas within the community borders. A = total pixels included in each political border.</p>
Description	IMP equals the number of built-up areas pixels divided by total pixels.
Units	% (0→100)

In Figure 1,2 and 3 the built-up density for Basel, Tyumen and Tel Aviv are displayed.

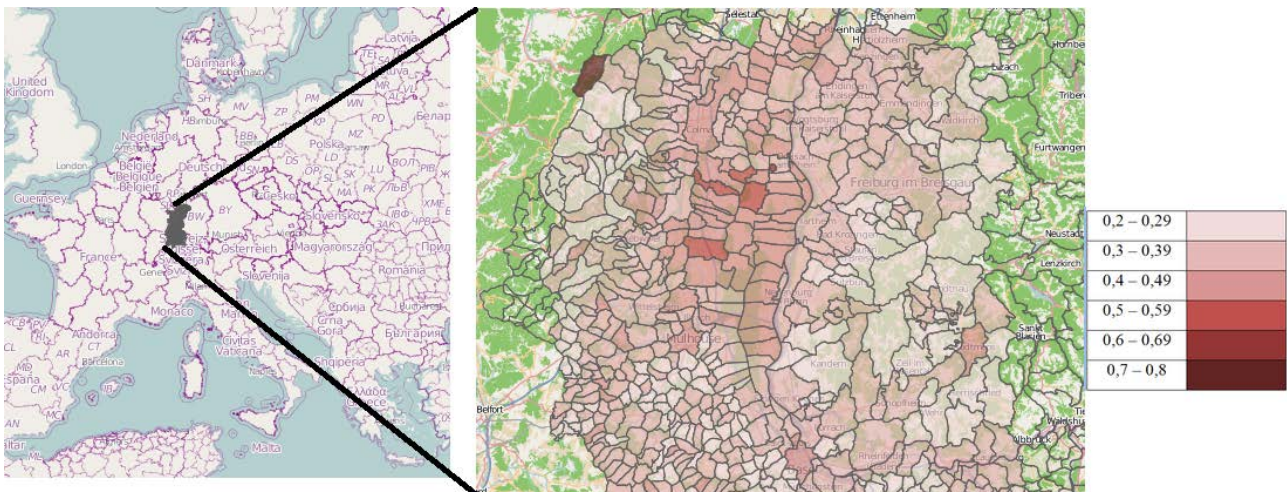


Figure 1. Built-up density in Basel – Switzerland

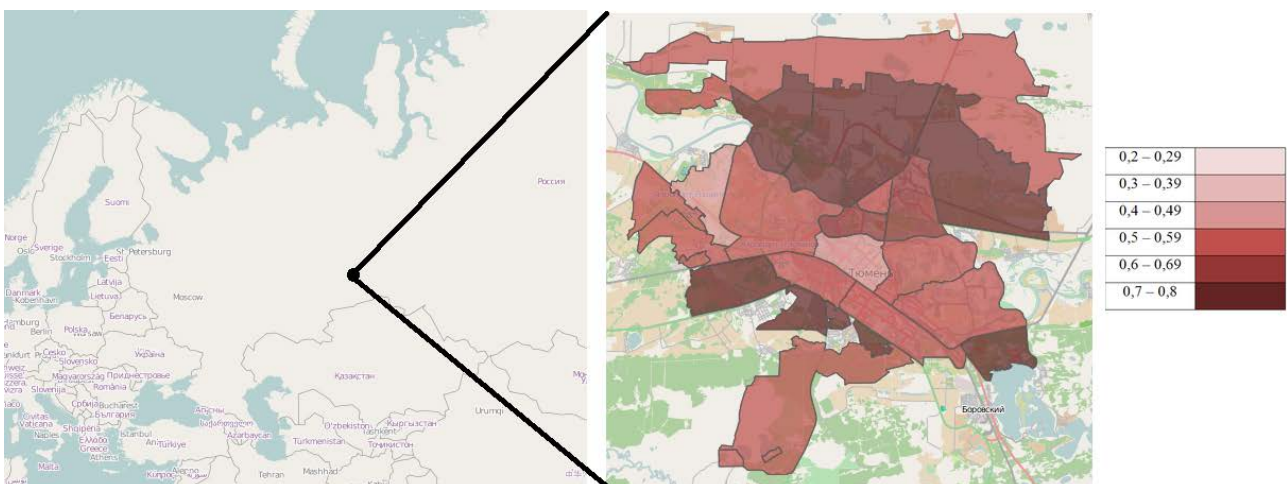
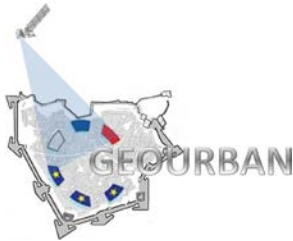


Figure 2. Built-up density in Tyumen – Russia



GEOURBAN

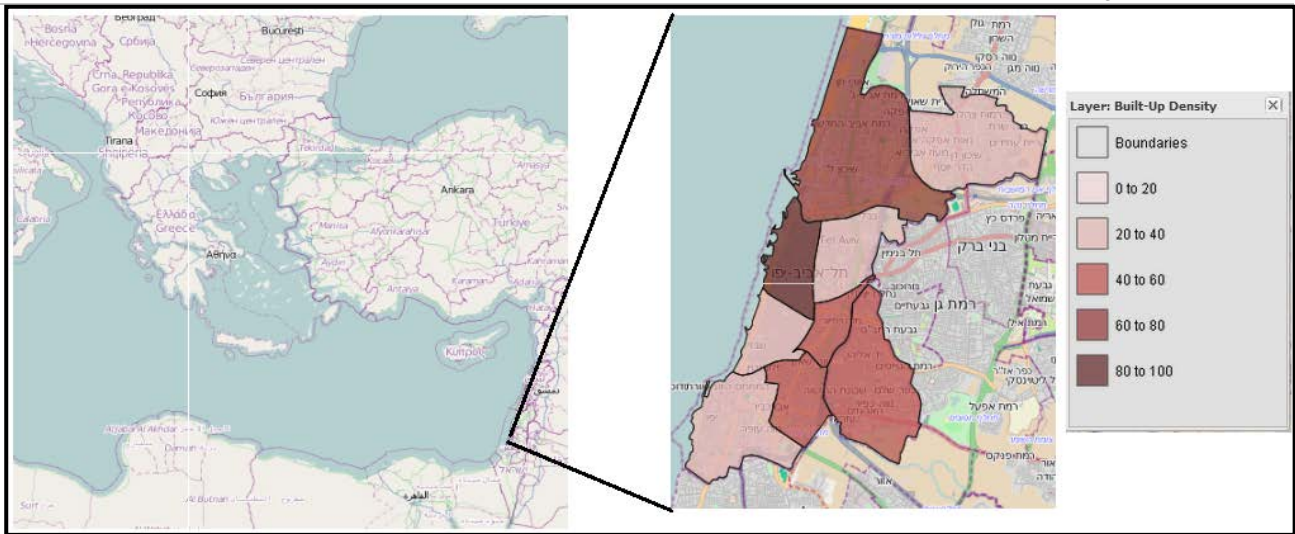


Figure 3. Built-up density in Tel Aviv - Israel

2.2.1.2. TerraSAR-X building density (TSX-building)

Synthetic Aperture Radar (SAR) technology is not as old as other optical systems technology. Advantages of spaceborne SARs include high spatial resolution, independence from illumination and weather conditions (data can be acquired day and night, with clouds or free of them). TerraSAR-X data (Werninghaus 2004) used in GEOURBAN allow the extraction of built-up areas in the level of individual buildings. Different techniques for building extraction have been applied in the literature, as described in the Deliverables D.4.2 and D.5.2. In the framework of GEOURBAN, the building density is provided as a TerraSAR-X product, with a color tone ranging from 0 to 255. 0 indicates high building density, while 255 values indicate the non building areas.

The urban footprint products from TerraSAR-X images were produced using resampling. The initial TerraSAR-X images were provided by DLR in 12x12m spatial resolution in a binary format (0: buildings, 255: non-buildings). These images were further analyzed using resampling method. Therefore, output images 30x30m were produced containing the density of building areas, ranging from 255 to 0 (low to high building density). The building density for Basel is given in Figure 4.

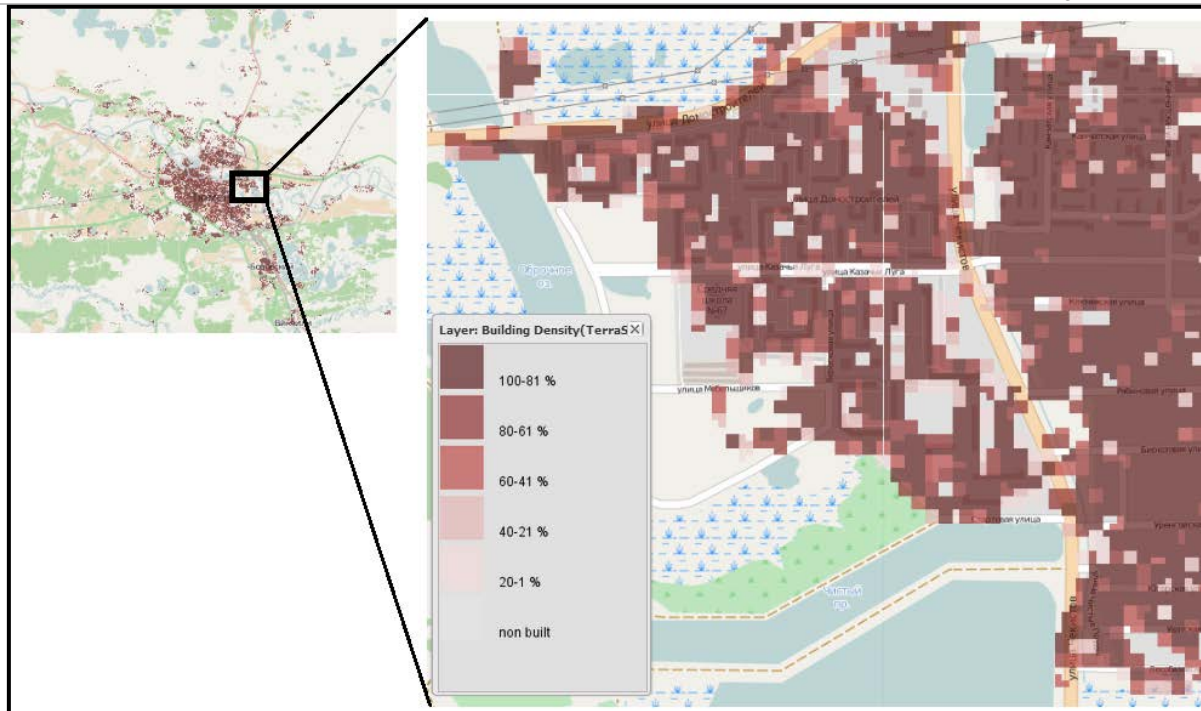


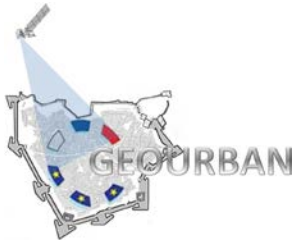
Figure 4. Building density derived by TerraSAR-X images for Basel

2.2.1.3. Open Space Density (OSD)

Open spaces in an urban environment provide many valuable services to residents, including recreational activities, aesthetic enjoyment and environmental functions (micro-climate stabilization and water purification). Open spaces refer to a number of land uses, such as green spaces (e.g. sports field), agricultural land and undeveloped land (Brander and Koetse, 2011). Open spaces become an important factor in improving urban life and its value increases with population density. More specifically, in dense residential places the indicator of open space density plays a powerful role in estimating the urban well-being.

In the current research project, Open Space Density (OSD) is calculated as the ratio between the pixels of open spaces and the total number of pixels within the political community boundaries. In our case, open spaces include grassland and agriculture.

Open space density is a measure of fragmentation of open spaces. Low values indicate fewer patches, while higher values indicate more patches of open spaces and therefore a higher spatial heterogeneity.



GEOURBAN

$OSD = \frac{N}{A}$	N = number of open spaces pixels within the community borders. A = total pixels included in each political border.
Description	OSD equals the number of open spaces pixels divided by total pixels.
Units	Net number (0→1)

In Figure 5 the maps of open space density for Basel and Tyumen are given.

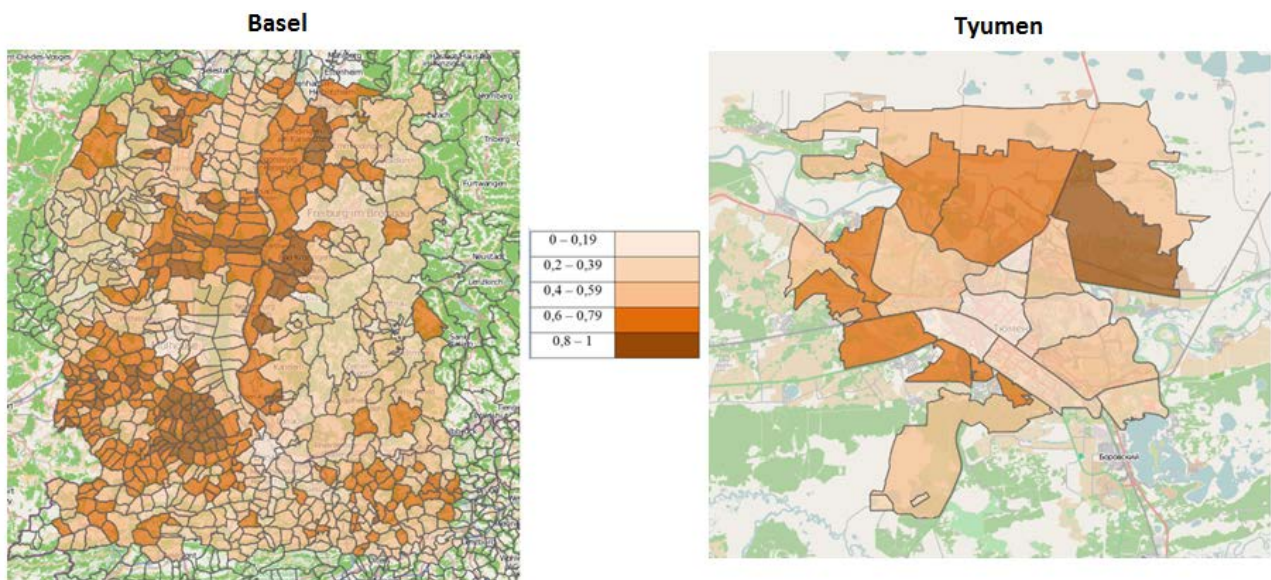
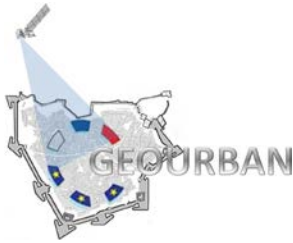


Figure 5. Open space density for Basel and Tyumen

2.2.1.4. Green Space Density (GSD)

The availability of attractive green spaces is a critical part of urban living. It is generally accepted that urban green spaces are essential for the health of citizens, making better standards of living. Urban planning pays much attention in preserving green areas and therefore, the indicator of green space density becomes an important tool in planners' requirements for "green liveability" (Herzele and Wiedemann, 2003)

Although green spaces can be considered as open spaces, in our case green spaces are examined as a separate indicator in order to give strength to areas with high green coverage. Therefore for our needs, green spaces are considered the forest and the grassland.



GEOURBAN

Green Space Density (GSD) is the ratio between the number of pixels of green spaces and the total number of pixels within the political community boundary.

Green space density is a measure of fragmentation of green spaces. Low values indicate fewer patches, while higher values indicate more patches of green spaces and therefore a higher spatial heterogeneity.

$GSD = \frac{N}{A}$	N = number of green spaces pixels within the community borders. A = total pixels included in each political border.
Description	GSD equals the number of green spaces pixels divided by total pixels.
Units	Net number (0→1)

In Figure 6 the green space density maps for Basel and Tyumen are presented.

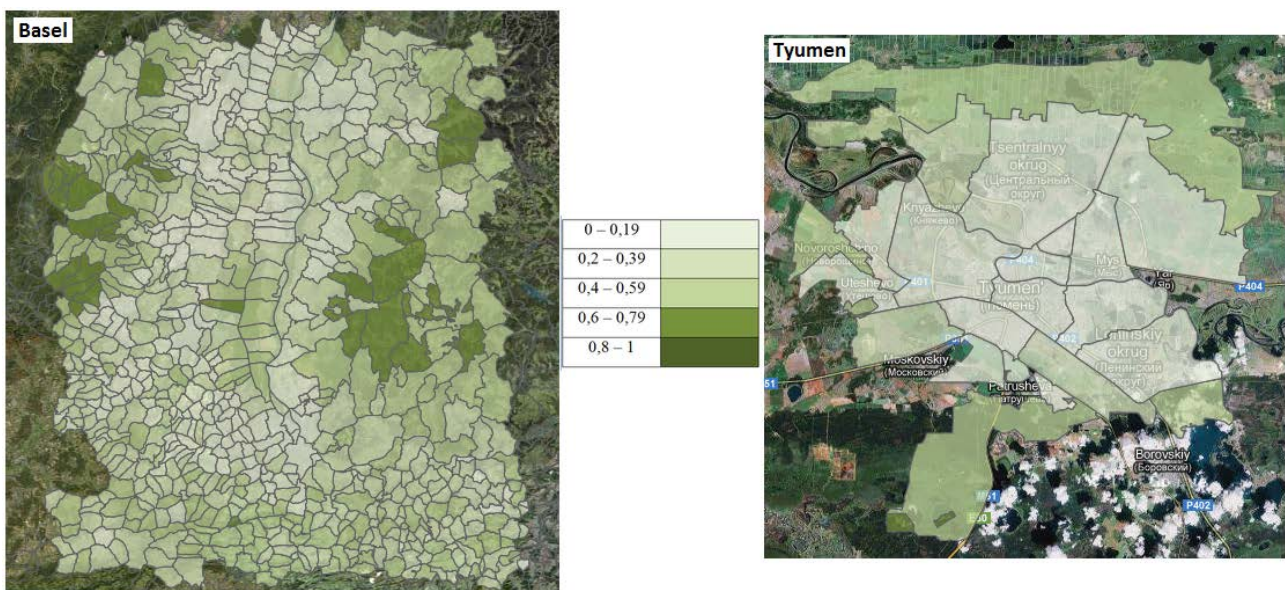
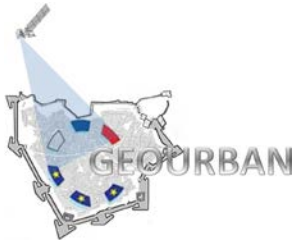


Figure 6. Green space density for Basel and Tyumen

2.2.2. Area / Edge Indicators

Area / Edge indicators consider both the complexity of the shape of the patches and their spatial distribution. For Edge Density, low values imply that there are relatively fewer and simpler patches of the specific land use, whereas large values imply that there are many complicated patches.



2.2.2.1. Edge Density (ED)

Edge Density of a class within administrative boundaries is the total length of the edge of patches divided by total area of administrative boundaries. As it is expected, in each class is assigned a value of ED and therefore, in each administrative boundary they exist as many ED as the classes of the land use map.

$ED = (\sum \frac{e_k}{A}) * 10000$	e_k = total length of edge of class k. A = total area of administrative boundary
Description	ED of a class equals the sum of the lengths of patches divided by total area of administrative boundary
Units	Meters per hectare

In Figure 7, the edge density for urban class in Basel area is presented.

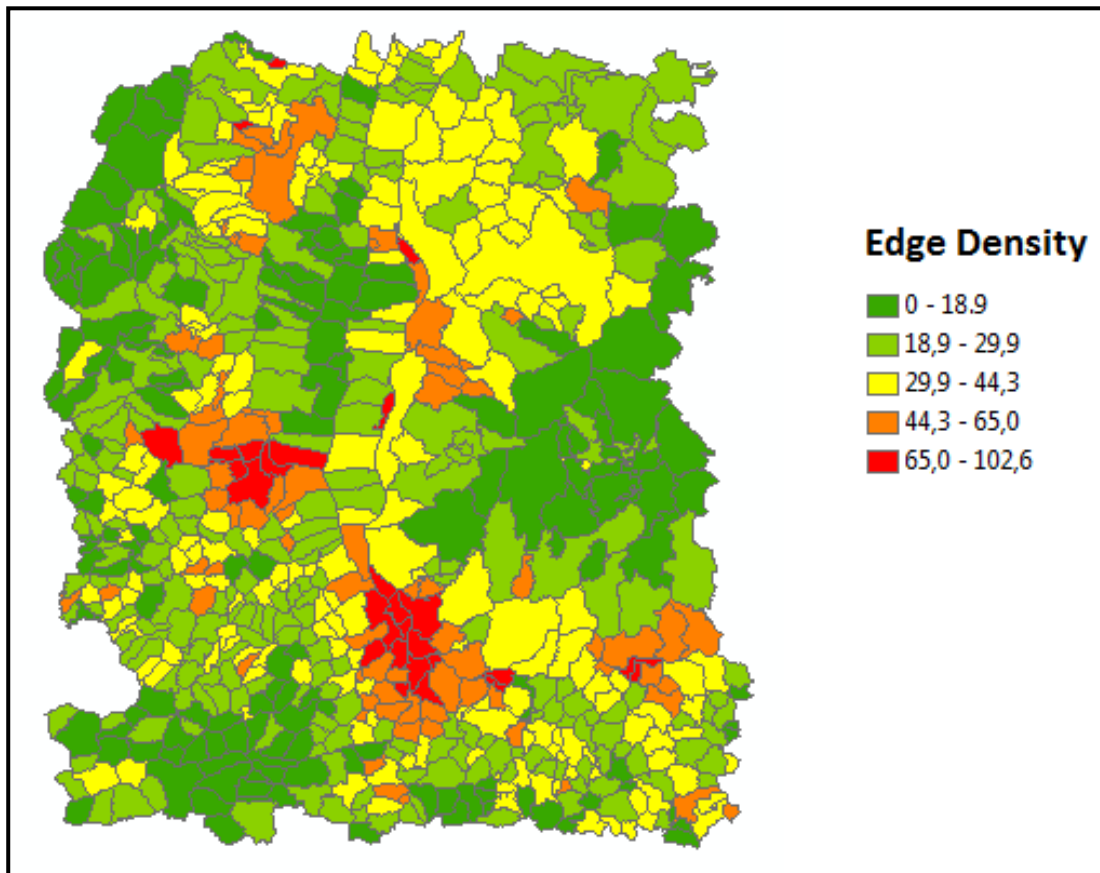
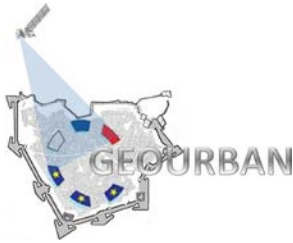


Figure 7. Edge Density for class: "urban" in Basel area



2.2.3. Ratio Indicators

Imperviouness-Open space ratio and Imperviousness – Green space ratio are two Ratio indicators, characterizing the analogy between different classes of landscape. Equally proportional volumes of corresponding classes produce ratio values close to 1.

2.2.3.1. Imperviousness-Open space Ratio (IOR)

Imperviousness-Open space Ratio (IOR) is an urban indicator which combines the built up density indicator with open space density indicator. High values of IOR indicate large impervious areas or small open space areas within an administrative boundary.

IOR= $\frac{\text{Imperviousness}}{\text{Open Space}}$	IOR is measuring the ratio between Imperviousness and Open Space
Description	IOR equals the Imperviousness which exist within a administrative boundary divided by the Open Space of this boundary
Units	Net Number

In Figure 8, the Imperviousness-Open space Ratio is presented for Basel area.

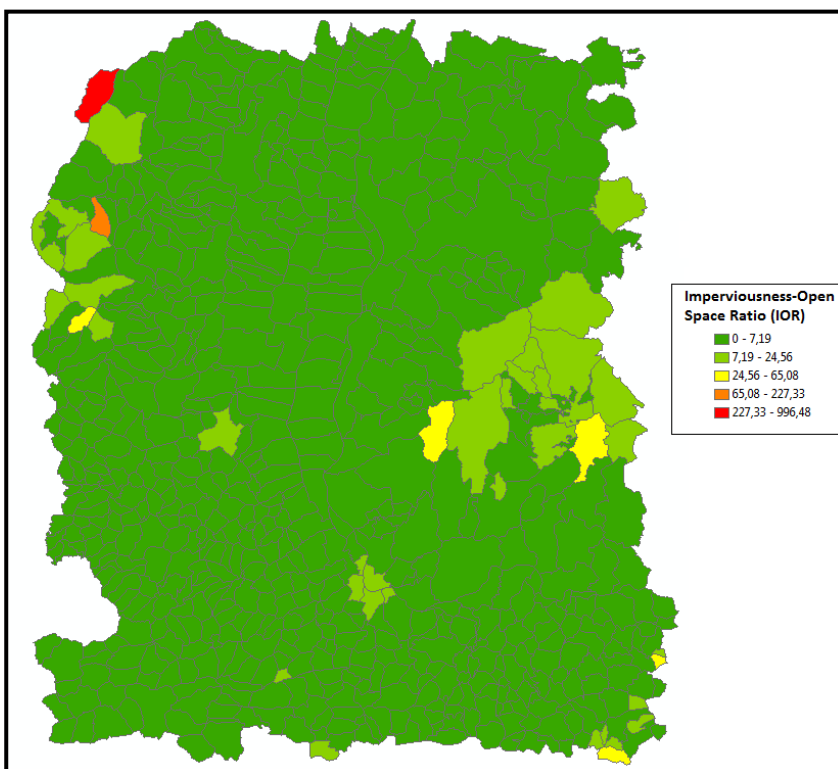


Figure 8. Imperviousness-Open space Ratio for Basel



2.2.3.2. Imperviousness-Green space Ratio (IGR)

Imperviousness-Green space Ratio (IGR) is a comparison of impervious and green areas which exist within an administrative boundary. High values of IGR indicate a urbanized areas with low green spaces.

IGR = $\frac{\text{Imperviousness}}{\text{Green Space}}$	IGR is measuring the ratio between Imperviousness and Green Space
Description	IGR equals the Imperviousness which exist within a administrative boundary divided by the Green Space of this boundary
Units	Net Number

In Figure 9, the Imperviousness-Green space Ratio for Basel is graphically presented.

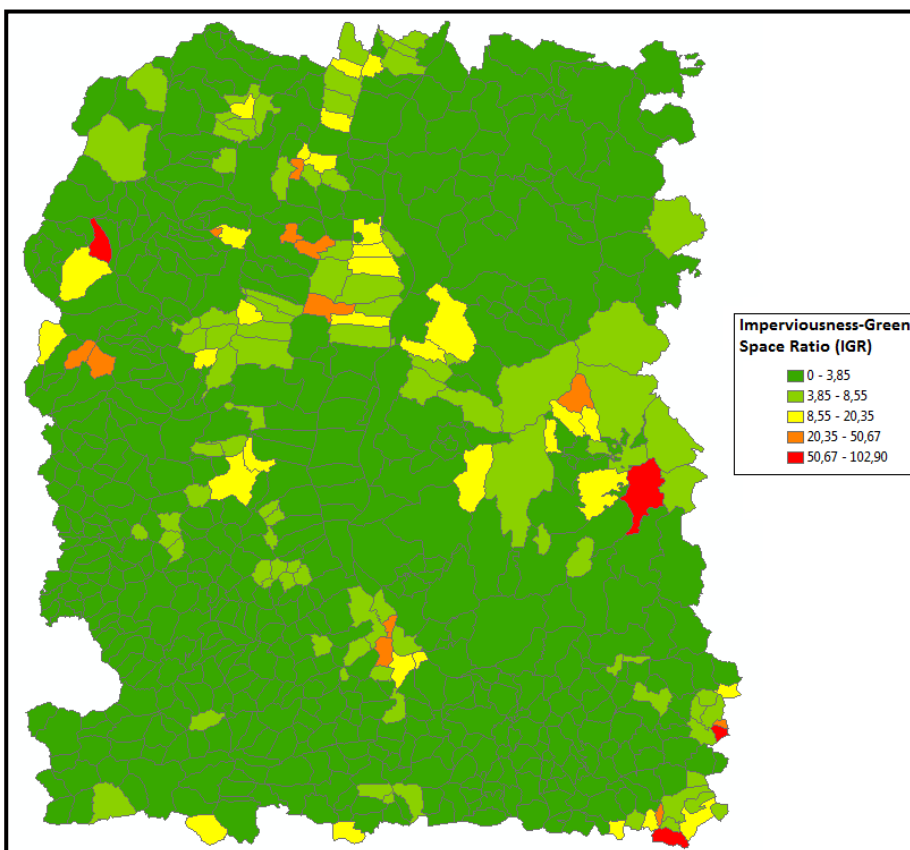
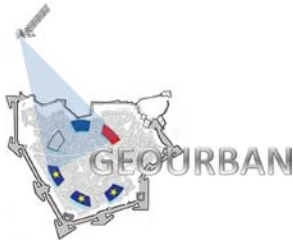


Figure 9. Imperviousness-Green space Ratio for Basel



2.2.4. Diversity Indicators

Diversity indicators are metrics of different patches (which belong to different land uses) in a landscape. They provide information about landscape composition, as well as rarity and commonness of patches. The ability to quantify diversity is an important tool for urban planners trying to understand urban structure.

2.2.4.1. Class Richness Density (CRD)

Class Richness Density is a measure of richness of different land cover classes within administrative boundaries. The more classes exist in an administrative boundary, the higher the CRD becomes. The Class Richness Density for Basel is presented in Figure 10.

$CRD = \frac{m}{A} * 10000$	m = number of classes within boundary A = total area of administrative boundary
Description	CRD equals the number of classes which exist within an administrative boundary divided by the total area of this boundary
Units	Number per hectare

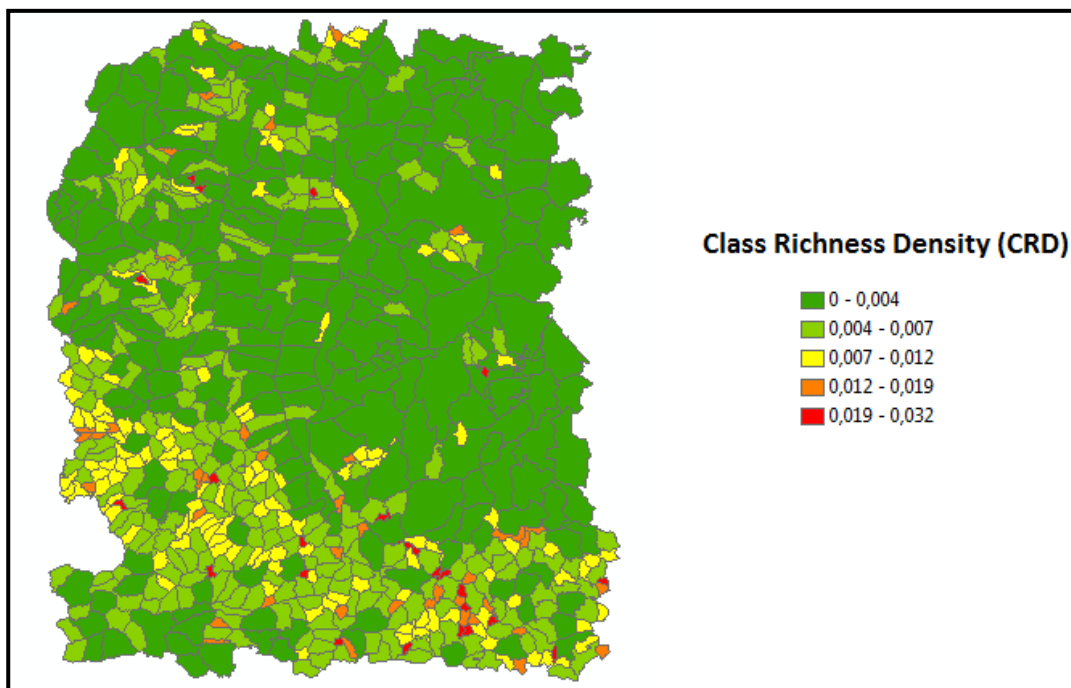
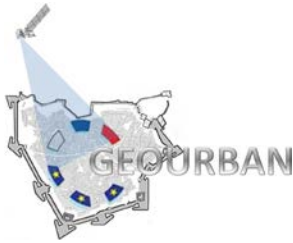


Figure 10. Class Richness Density for Basel



2.2.4.2. Ecological Effectiveness Ratio (EER)

The Biotope Area Ratio (BAR) was first developed in the late 80s to measure the ecological value of urban areas in West Berlin, Germany. As a tool in environmental planning and management, BAR provided support to decision making process especially in urban ecology. Since then, several modifications of BAR have been made for a better adaptation to specific circumstances (Lakes and Kim, 2012). In our study the Ecological Effectiveness Ratio (EER) was used, which can be calculated using the following formula:

$$EER = \frac{\text{ecologically-effective surface areas}}{\text{total land area}}$$

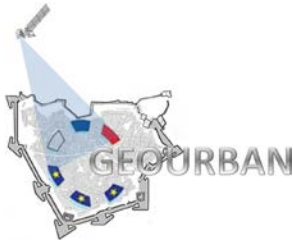
The EER is the ratio of the ecologically effective surface area to the total land area. The ecologically effective surface area is the result of combining the areas of different ecological parts of the study area, where for each part a weight is suitably assigned. The different ecological parts take a weight according to their ecological value (Table 2, Lakes and Kim, 2012).

The calculation of EER in our study areas, concerning the surface type and the corresponding weighting factor is based on Table 3.

Surface type		Weighting factor
Forest	▶	1
Water	▶	1
Agriculture	▶	0.5
Grassland	▶	0.7
Residential I, II, III	▶	0
Industrial	▶	0


Table 2. Surface types and weighting factors for Basel, Tyumen and Tel Aviv

The equation for Ecological Effectiveness Ratio (EER) calculation is given below:



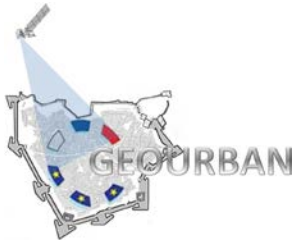
GEOURBAN

$EER = \frac{\sum \text{Surface type} * \text{weighting factor}}{A}$	<p>Surface type: m² of the land type within the examined political boundary</p> <p>A = m² included in each political boundary.</p>
Description	EER estimates the ecological value in a specified area.
Units	Net number (0→1)

Surface type	WR Berlin	WR Seoul	Description of surface types
 Sealed surfaces	0.0	0.0	Surface is impermeable to air and water and has no plant growth (e.g., concrete, asphalt, slabs with a solid sub-base)
 Partially sealed surfaces	0.3	0.2	Surface is permeable to water and air; as a rule, no plant growth (e.g., clinker brick, mosaic paving, slabs with a sand sub-base)
 Semi-open surfaces	0.5	0.5	Surface is permeable to water and air; infiltration; plant growth (e.g., gravel with grass coverage, wood-block paving)
 Permeable pavement	-	0.3	Surface is permeable to water; no plant growth (e.g. gravel or sand paving on natural ground)
 Surfaces with vegetation, unconnected to soil below	0.5	0.5	Surfaces with vegetation on cellar covers or underground garages with less than 80 cm (Berlin), 90 cm (Seoul) of soil covering
 Surfaces with vegetation, unconnected to soil below	0.7	0.7	Surfaces with vegetation that have no connection to soil below but with more than 80 cm (Berlin), 90 cm (Seoul) of soil covering
 Surfaces with vegetation, connected to soil below	1.0	1.0	Vegetation connected to soil below, available for development of flora and fauna
 Rainwater infiltration per m ² of roof area	0.2	0.2	Rainwater infiltration for replenishment of groundwater; infiltration over surfaces with existing vegetation
 Vertical greenery < 10 m (height)	0.5	0.3	Greenery covering walls and outer walls with no windows; the actual height, up to 10 m, is taken into account
 Greenery on rooftop	0.7	0.5	Extensive and intensive coverage of rooftop with greenery, regulation of the soil depth (≥10 cm) in Seoul
 Permeable water surface	-	1.0	Water area, water can run through the soil below (e.g. natural pond)
 Impermeable water surface	-	0.7	Water area, water cannot run through the soil below (e.g. artificial pond)

Source: SenStadt (2011), Seoul 2004.

Table 3. Types of surfaces and weighting ratios for Berlin and Seoul (Lakes and Kim, 2012)



2.3. Urban Surface Type

The urban surface type indicators include: Imperviousness (from RapidEye data), Fractional Land Cover, Surface Albedo and Surface emissivity.

2.3.1. Imperviousness

RapidEye system provides EO imagery in a spatial resolution of 5 meter. RapidEye data can be retrieved by five identical satellites, collecting over 4 million Km² of 5-band color imagery every day. RapidEye data are very attractive form of geospatial information because of the ability to have almost daily coverage of any spot on earth surface, covering the entire world in 13-day frequency (Melese et al. 2007).

The approach applied on RapidEye data consists of an object-based procedure with two modules: segmentation and classification. The basic task of the segmentation is to merge homogenous pixels into single segments in order to differentiate between heterogeneous neighboring regions (Benz et al. 2004). In the classification phase the band ratio 'normalized difference vegetation index' (NDVI) is first used to mask natural environment areas. Then, for each segment different features (i.e., size, shape and spectral information) are extracted and provided as input to a fuzzy classifier, which provides as output a probability of class membership. If such probability is higher than a certain threshold, then the object is categorized as belonging to the urban class.

Imperviousness from Basel is displayed in Figure 11.

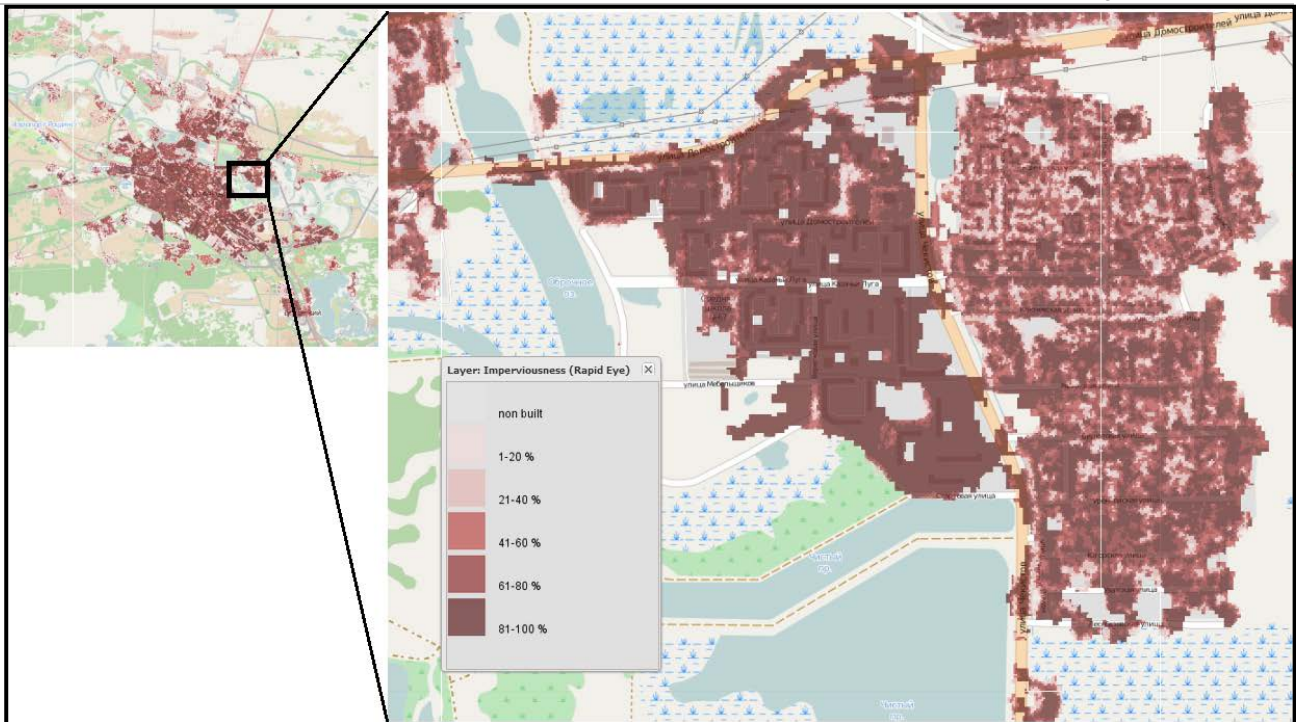
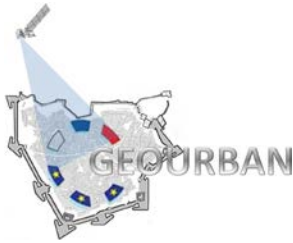


Figure 11. Imperviousness derived by RapidEye data for Basel

2.3.2. Fractional Land Cover

Fractional land cover refers to the proportion of a pixel by predefined land cover types. The estimation of fractional cover is called “spectral unmixing” and the proportions of each land cover in a pixel should sum to one. A Linear Spectral Mixing Analysis technique (Adams et al, 1995) was employed used in GEOURBAN. According to this method, the spectrum which returns to the sensor is a linear combination of all the components spectra within a pixel (Lu and Weng, 2006). These components are called end-members. The selection of endmembers is usually an image-based process, where endmembers can be easily obtained from the extreme purest pixels of the image. The band scatterplots are very useful in defining pure class pixels. The Pixel Purity Index (PPI) was used for selection the purest pixels. According to the PPI, pure pixels were selected for two dominant classes in Tyumen: vegetation and imperviousness. Therefore, the final fractional land use map is an image where each pixel contains a proportion of imperviousness and vegetation.

Figure 12 presents the fractional land cover for Tyumen, as derived by Landsat imagery, using ENVI software.

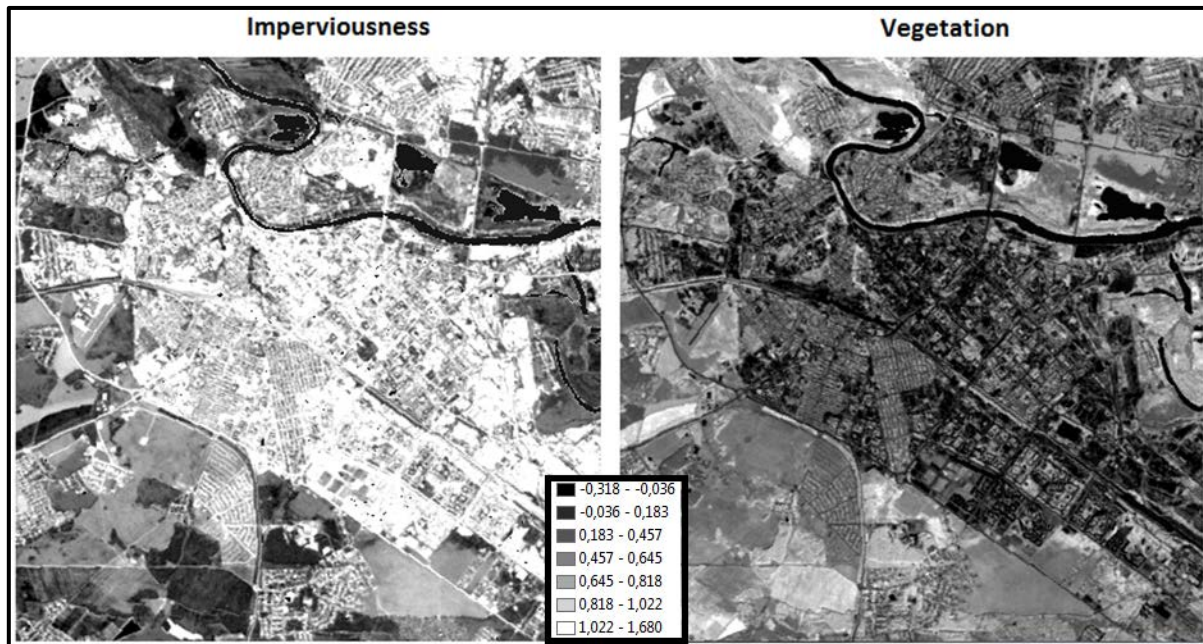
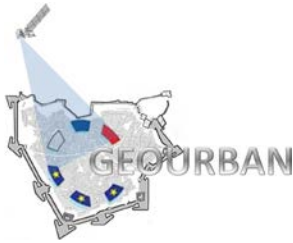


Figure 12. Fractional land use map for Tyumen (Imperviousness - Vegetation)

2.3.3. Surface Albedo

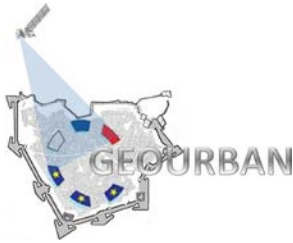
The surface albedo is the diffuse reflectivity (reflecting power) of a surface and it expresses the ratio of reflected radiation from the surface to incident radiation upon it. The values of the surface albedo ranges from zero (no reflection – black body) to 1 (perfect reflection – white surface). The urban surface broadband albedo is important for urban energy balance. Among several types of broadband albedos the total shortwave albedo covering the wavelength range from about 0.4...2.5 μm is of main interest for urban planning purposes. The GEOURBAN surface broadband albedo product was calculated by Landsat narrowbands applying the conversion algorithm for Landsat TM/ETM+ surface spectral reflectance as published by Liang (2000). The results of this conversion have been validated in Liang et al. (2002) and have been shown to be accurate.

Narrowband to broadband conversion formula for Landsat TM/ETM+ after Liang (2000):

$$\alpha = 0.356 \alpha_1 + 0.130 \alpha_3 + 0.373 \alpha_4 + 0.085 \alpha_5 + 0.072 \alpha_7 - 0.0018$$

with: α total shortwave albedo

α_x spectral surface reflectance of TM/ETM+ band x



GEOURBAN

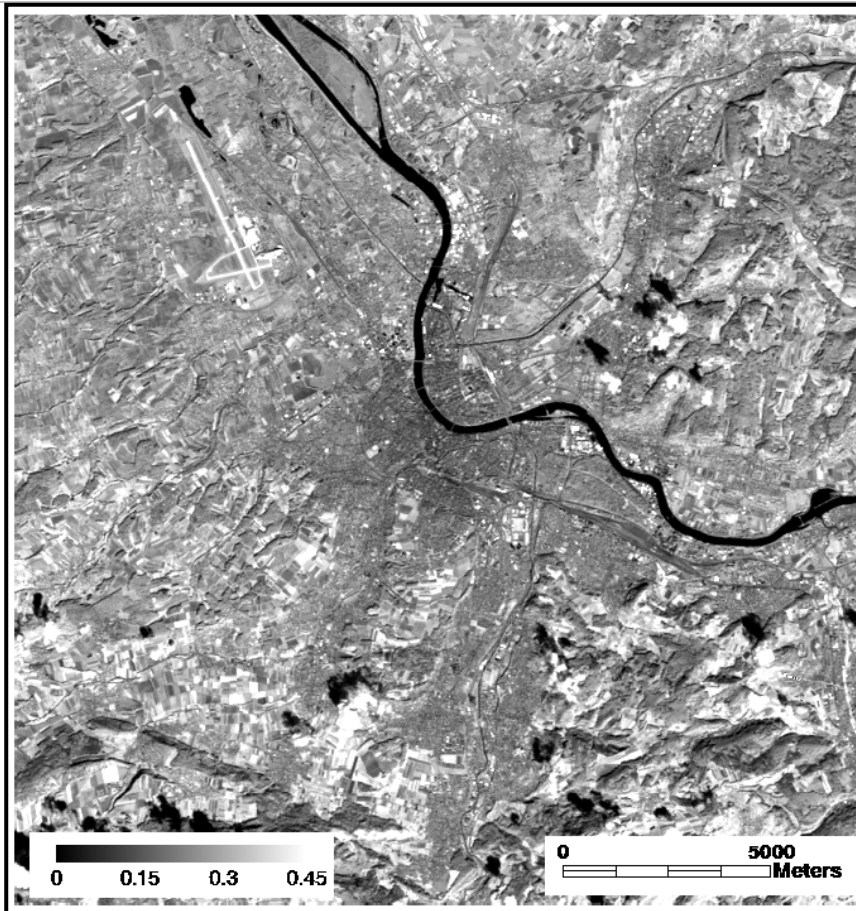
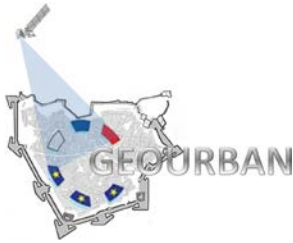


Figure 13. Broadband albedo for Basel (2011)

Surface Albedo can be also estimated from white-sky (completely diffuse) and black-sky (direct beam) albedo products as retrieved from MODIS observations (Schaaf et al. 2002). MODIS observations do not directly measure surface albedo. Spectral albedo is derived by directional integration of land surface reflectance recorded at the sensor and is therefore dependent on the Bidirectional Reflectance Distribution Function (BRDF), which describes the dependency of reflectance on view and solar angles. The MODIS BRDF/albedo algorithm makes use of a kernel-driven, linear BRDF model which relies on the weighted sum of an isotropic parameter and two kernels (volumetric and radiometric) of viewing and illumination geometry to determine reflectance (Schaaf et al. 2002).

The black-sky and white-sky albedo are computed using polynomial expressions of the kernel weights, as described by Schaaf et al. (2002). The wavelength, the optical depth, the aerosol type and the terrain can be used for diffuse component calculation. Therefore, for partially diffuse illumination the actually occurring, the spectral albedo may be approximated as a linear combination of the limiting cases. For this approximation, the



fraction of diffuse radiation should be calculated; its calculation is straightforward as a function of solar zenith angle and AOT.

2.3.4. Surface emissivity

The surface emissivity is the relative ability of a surface to emit energy by radiation and equals to the ratio of energy radiated by the energy radiated by a black body at the same temperature. The surface emissivity of a black body is 1, while any real object has emissivity lower than 1. The more reflective a surface is, the lower the emissivity is.

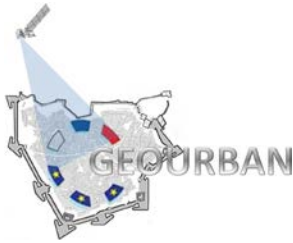
The emissivity of land surface varies with vegetation, surface moisture, and roughness. Emissivity not only depends on the surface type but also on its physical condition imposing additional large temporal changes. There are several methods for the estimation of land surface emissivity (LSE) derived from satellite data. In GEOURBAN, we estimated the LSE from the Normalized Difference Vegetation Index (NDVI). In the frame of GEOURBAN, of the several studies that propose this approach, we favour the application of the NDVI threshold method (NDVI^{THM}) described in Sobrino et al. (2004), because it fully covers our needs in terms of accuracy and operability.

The NDVI^{THM} algorithm is basically a case-by-case analysis of the NDVI. The different cases are:

- NDVI < 0.2: pixel considered as bare soil, $\epsilon = 0.97$
- NDVI > 0.5: pixel considered as fully vegetated $\epsilon = 0.99$
- $0.2 \leq \text{NDVI} \leq 0.5$: pixel considered as a mixture of bare soil and vegetation, ϵ is calculated as follows: $\epsilon = 0.004 * \text{PV} + 0.986$, where PV is the vegetation fraction of the pixel according to Carlson and Ripley (1997):

$$P_V = \left[\frac{\text{NDVI} - \text{NDVI}_{\min}}{\text{NDVI}_{\max} - \text{NDVI}_{\min}} \right]^2, \text{ with } \text{NDVI}_{\min, \max} \text{ as } 0.2 \text{ and } 0.5, \text{ respectively.}$$

Moreover, daily emissivity maps (MODIS Level 2 emissivity product) are available as global maps at 1 km spatial resolution. The classification-based emissivity method proposed by Snyder et al. (1998) is used as developed with the linear BRDF models. Such models utilize spectral coefficients derived from laboratory measurements (Salisbury & D'Aria 1992, 1994) of material samples. They also use structural parameters as derived



from approximate descriptions of the cover type (Snyder & Wan 1998). Surface emissivity can be also estimated with high resolution satellite data taking into account the 'mixed pixels' problem and the emissivity angular anisotropy (Mitraka et al. 2012).

2.4. Urban Sprawl

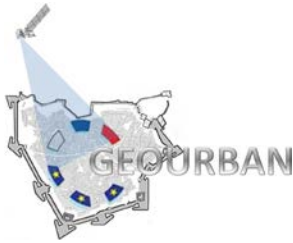
Urbanization usually leads to an undesirable growth, called urban sprawl. Urban sprawl has one or more of the following characteristics: non-compact growth, low density suburban development, scattered or random linear development and strip or ribbon structure (Wassmer 2000; Ewing 2008). Urban sprawl has negative impact in cities because of high and unsustainable energy consumption and increased use of cars and heating, the reduced level of means of transportation in the suburbs and the fragmentation of urban development (CEC 2006, 2011). The reduction of urban sprawl not necessarily implies reduction of urban expansion, but poses some rules in this, that it becomes more functional.

The GEOURBAN urban sprawl indicators are: Urban Fringe, Scatter Development and Change Detection.

2.4.1. Urban Fringe

The urban fringe is a measurement of sprawl and is defined as the built up areas which have neighborhoods that are 30-50% built up.

$UF = \text{Built up}_{\text{neighb}=30-50\% \text{ built up}}$	UF is measuring the urban sprawl and compactness
Description	UF equals the built up areas within the administrative boundaries which have neighborhoods with 30-50% built up
Units	m ²



The urban fringe for Basel is given in Figure 14.

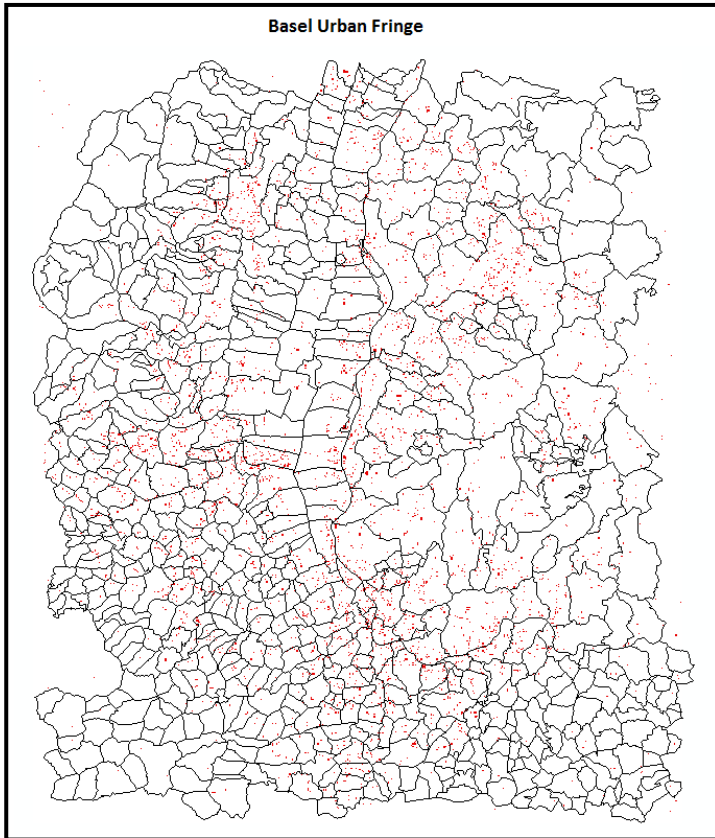
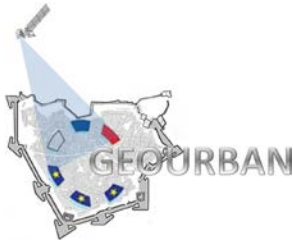


Figure 14. Basel Urban Fringe

2.4.2. Scatter Development (SD)

Scatter Development is another measurement of sprawl which describes the built up areas which have neighborhoods that are less than 30% built up.

SD = Built up _{neighb=<30% built up}	SD is measuring the urban sprawl and compactness
Description	SD equals the built up areas within administrative boundaries which have neighborhoods < 30% built up
Units	m ²



The size of neighborhood can be set at 500m. The scatter development for Basel is presented in Figure 15.

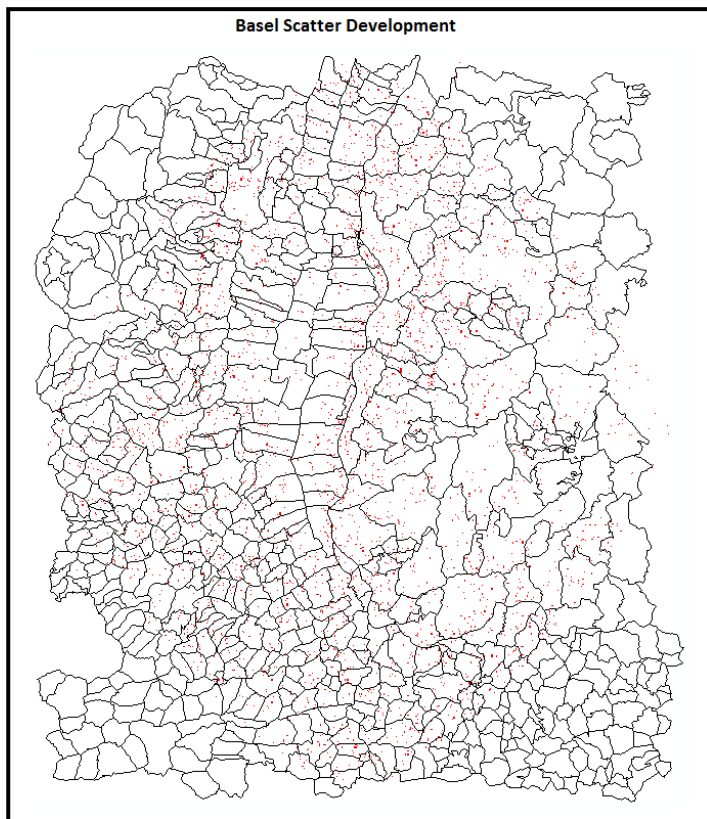
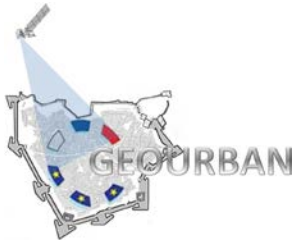


Figure 15. Basel Scatter Development

2.4.3. Change Detection

Change detection is the process where identification of the differences of a phenomenon is taken place within a time interval. EO data are more suitable for change detection comparing with other data sources because of the repetitive coverage at short time intervals. Nowadays, urban land uses change rapidly due to social, economic and environmental forces and there is a definite need of applying change detection methods in comparing earth observation data of the same area at different times (Ridd and Liu, 1998). Therefore, change detection of urban land uses is of great importance in urban planning and management, because it provides to urban planners a clear representation of urban growth, identifying the areas of rapid change which need special treatment.



Many algorithms have been developed in order to address change detection problems. Some of them include image overlay, image differencing, image regression, image rotating, principal component analysis, vegetation index differencing and change vector analysis (Singh 1989, Afify 2011).

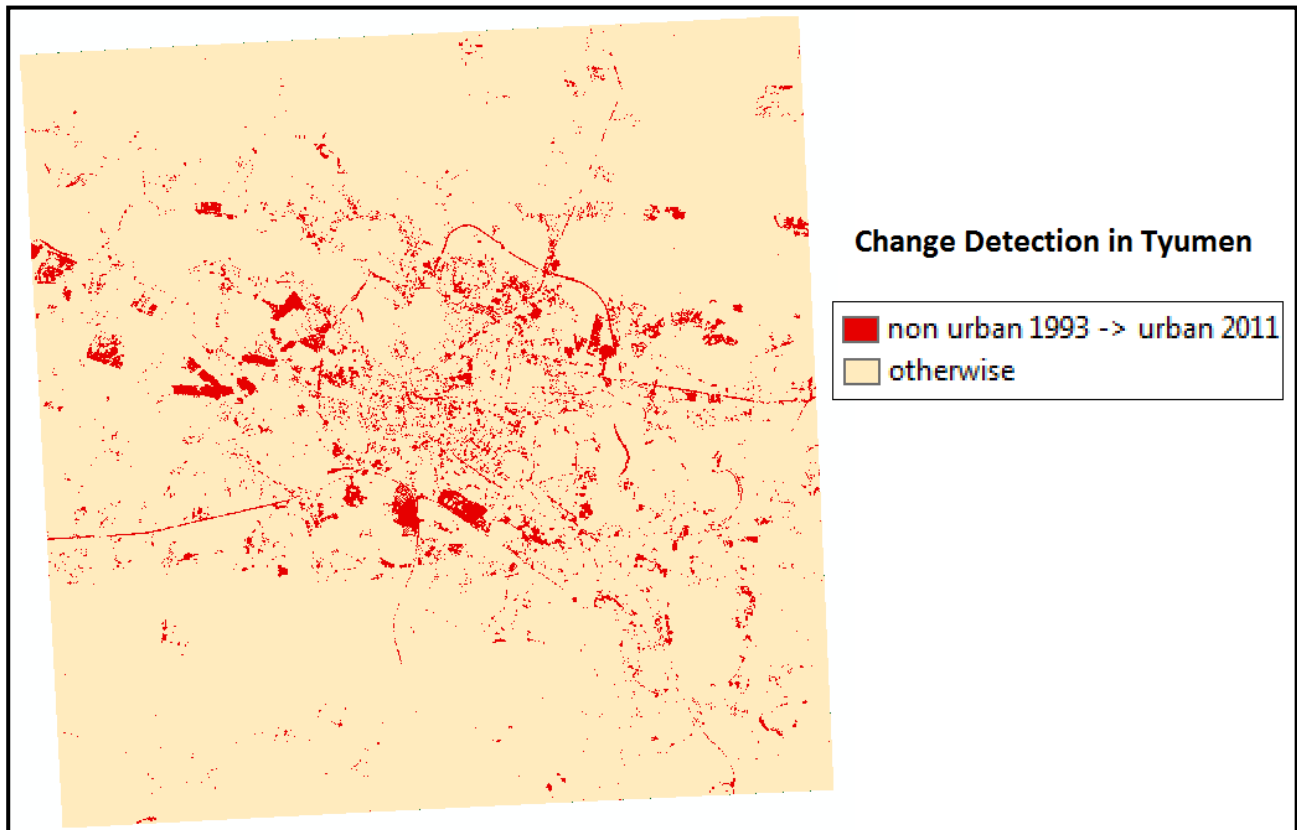
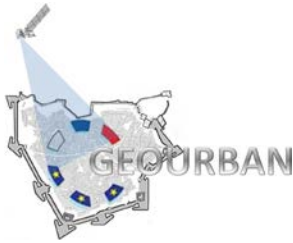


Figure 16. Change Detection in Tyumen for urban land use class between 1993 and 2011
GEOURBAN change detection tasks focused on Basel and Tyumen. Land use maps for 1984 and 2011 in Basel were produced. In Tyumen, 1993 and 2011 land use maps were also produced. The change detection was focused in urban land use changes and therefore, the non-urban areas which became urban were detected (Figure 16).

2.5. Urban Environmental Quality

The GEOURBAN Urban Environmental Quality indicators are: Surface Urban Heat Island and Aerosol Optical Thickness.

2.5.1. Surface Urban Heat Island



GEOURBAN

SUHI intensity describes the difference in surface temperature between a conurbation and the surrounding rural area. Urban geometry, compactness, population, land use and vegetation cover influence urban heat island (Tomlinson et al, 2012). The surface temperature is of high importance to the study of urban climate and urban environmental quality, because it helps us to better understand the urban environment and their impact to human beings.

Satellite systems with thermal infrared radiometers acquire thermal infrared observations, which can be used to derive the Land Surface Temperature (LST), by means of inversion modeling, as described in the Deliverable D.5.2. Systems like MODIS (Moderate Resolution Imaging Spectroradiometer), onboard Terra and Acqua satellites, acquire daily thermal infrared data, which are automatically processed by inversion algorithms accounting for emissivity and atmospheric effects (Wan et al. 2004, Tran et al. 2006) and producing daily LST products. These products are on-line available at 1 km x 1 km spatial resolution in Hierarchical Data Format (HDF) (<http://earthexplorer.usgs.gov/>). Despite its low spatial resolution, the MODIS LST product is acceptable in SUHI studies, because of its high temporal resolution (two images daily per satellite).

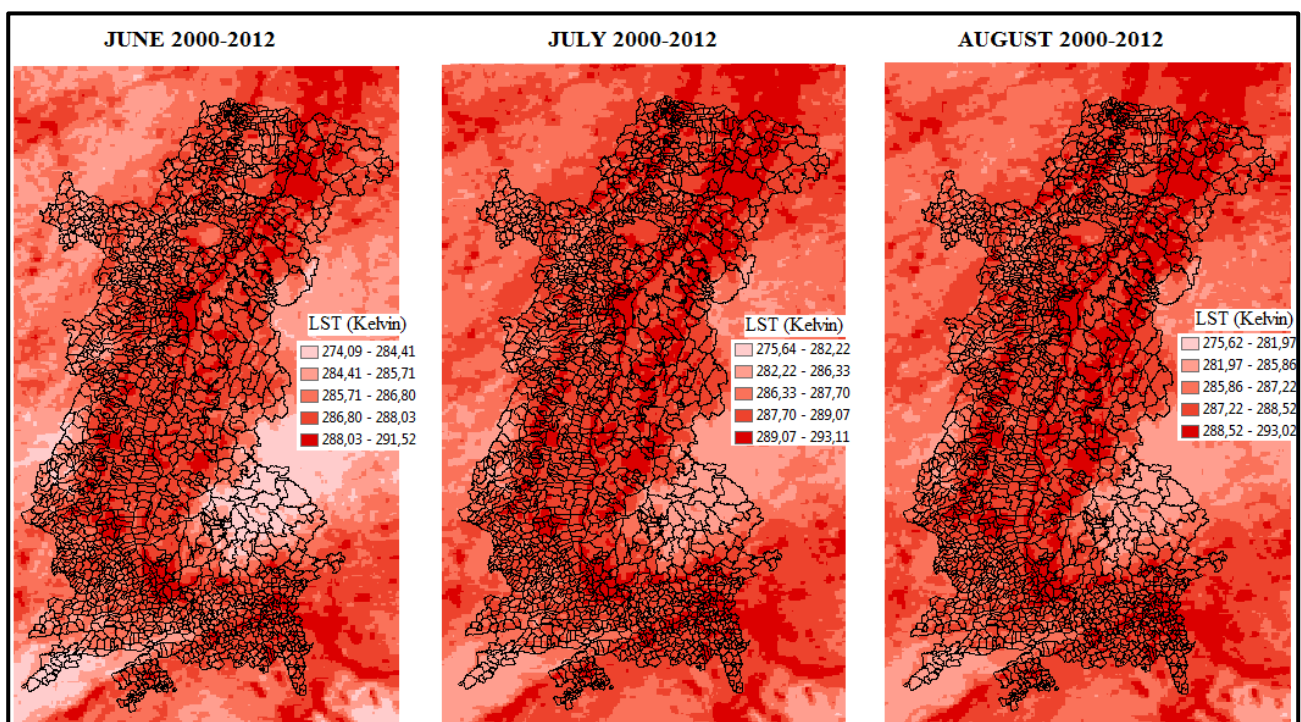
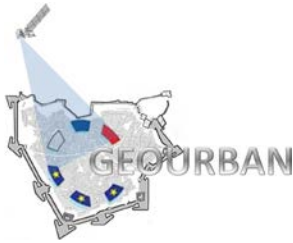


Figure 17. Average monthly LST (Kelvin) for 13 years in Basel



In Figure 17 an example of MODIS derived nighttime LST distribution of Basel is presented. The respective LST products were downloaded in HDF format and the Digital Numbers of the respective images were de-scaled (multiplied by 0.02) to derive LST (in Kelvin).

2.5.2. Aerosol Optical Thickness (AOT)

MODIS Level 2 is a category of higher level products, available on a daily basis, including the Aerosol Product, which monitors aerosol properties. The most updated and validated MODIS Level 2 Collection (C051) comprises of HDF files of all products, spanning the entire Terra and Aqua operational periods (February 2000 and July 2002 until present, respectively) are on-line available (<http://ladsweb.nascom.nasa.gov/data/search.html>). While Collection 6 is the latest available, Collection 5.1 is the latest Collection which has been thoroughly validated, as far as aerosol parameters are concerned.

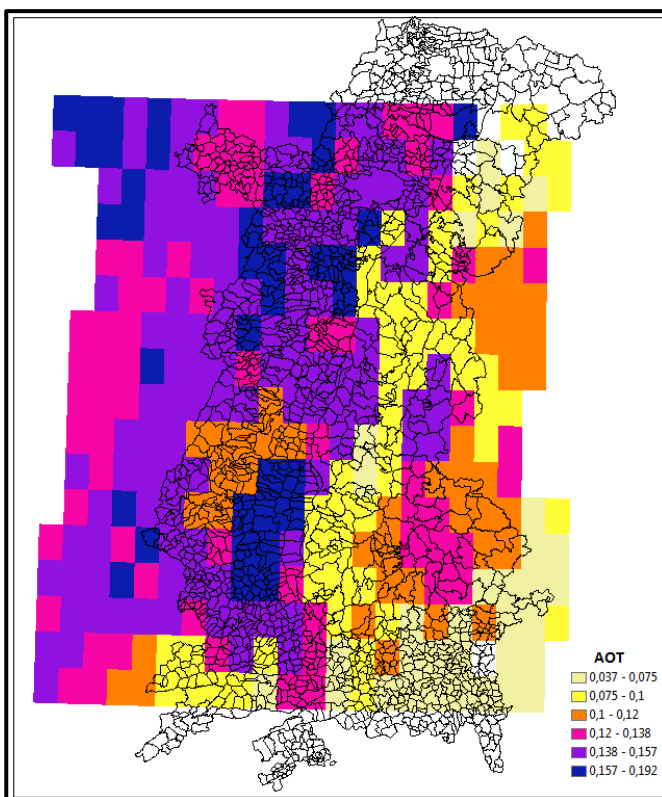
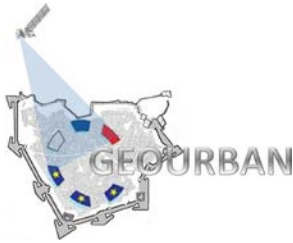


Figure 18. AOT values for Basel (MODIS 2012 image)

The Aerosol Optical Thickness (AOT) is an important aerosol parameter included in this product. The MODIS derived daily AOT at 10 km x 10 km is used in GEOURBAN. A



variety of programs (e.g. Matlab, HEGTool) can be used to reproject and descale the respective Digital Numbers to AOT values for each pixel. In Figure 18, the AOT map is given for the Basel area.

2.6. Vulnerability to Hazards

2.6.1. Accessibility to critical services

The vulnerability to natural hazards should be carefully assessed in urban areas because people need should be safe in the environment they live. Droughts, floods, earthquakes and other natural hazards have become frequent and therefore, disaster response plays an important role in case of emergency. Accessibility to critical services is an indicator of the environmental vulnerability.

In GEOURBAN, the distance of specific points of critical infrastructure is considered to assess the vulnerability of each area. Therefore, distance maps of specific points of interests such as hospitals were prepared.

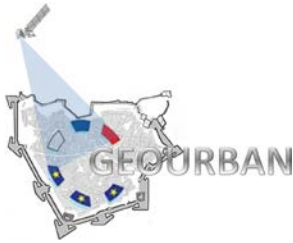
In Figure 19, the distance from the critical services (hospitals) is presented as an example.

2.7. Socioeconomics

2.7.1. Exposure to PM

Particulate Matter (PM) of both fine (PM_{2.5}) and coarse (PM₁₀) particles is used as an indicator of environmental quality in urban areas. PM have serious effects on human health, increasing morbidity and mortality. Respiratory problems, cardiovascular diseases and decreased birth weights and lengths are some of the negative PM impact in human life.

PM monitoring is based primarily on ground measurements, which their spatial and temporal coverage is highly variable. Therefore, PM estimation using satellite remote sensing techniques is more than appropriate. The Aerosol Optical Thickness (AOT) is the most common satellite derived parameter used for PM estimation (Benas et al. 2013).



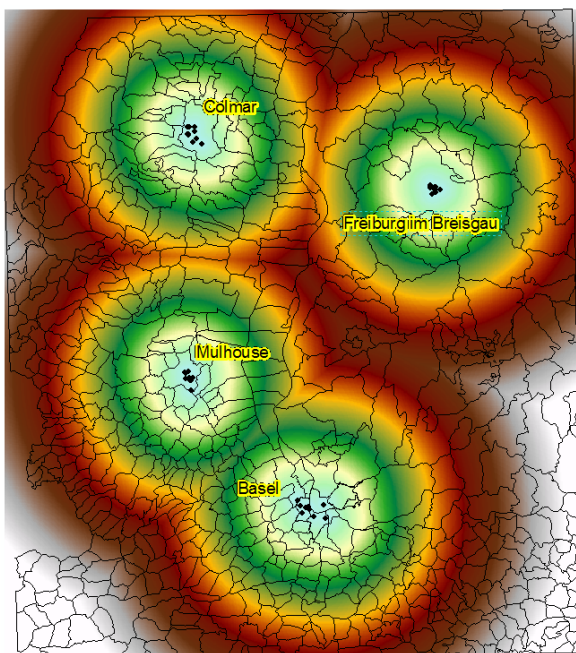
GEOURBAN

One of the several methods for PM estimation is the multiple regression analysis technique, which is based on satellite derived AOT and other related parameters, such as surface temperature and relative humidity. All parameters are available from the Moderate Resolution Imaging Spectroradiometer (MODIS) sensors on board NASA's Terra and Aqua satellites at 5 km x 5 km spatial resolution (MODIS Level 2 Atmosphere Products). AOT is also available from MODIS Level 2 products at 10 km _ 10 km spatial resolution. The regression equation can be written as follows (Benas et al. 2013):

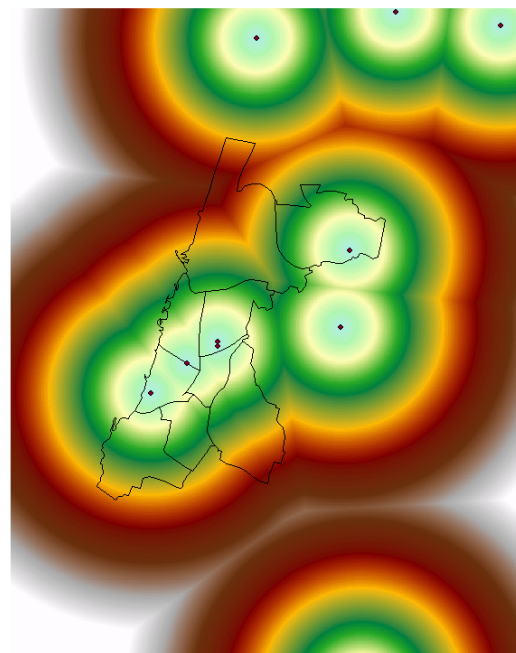
$$PM_{10} = b_0 + b_1 AOT + b_2 RH + b_3 STMP + \epsilon,$$

where RH is the relative humidity and STMP is the surface temperature, ϵ is the error variable and b_x are the regression coefficients.

A large fraction of urban population is exposed to levels of PM₁₀ in excess of threshold values set for the protection of human health. Exceedance days are defined as days with PM₁₀ 24-hours average above 50 mg/m³ according to European Environmental Agency. Exposure to PM₁₀ is the annual population average exposure to air pollution by PM₁₀.



Basel



Tel Aviv

Tyumen

Figure 19. Accessibility to critical services (hospitals) in Basel and Tel Aviv.